



New two-photon absorption benzotriazole–coumarin dyads: the evidence of internal proton transfer in the excited state



Yulong Gong, Yao Lu, Zhenqiang Wang, Shengtao Zhang, Ziping Luo*, Hongru Li*, Fang Gao*

College of Chemistry and Chemical Engineering, Chongqing University, Chongqing 40044, China

ARTICLE INFO

Article history:

Received 15 August 2014

Revised 14 November 2014

Accepted 17 November 2014

Available online 21 November 2014

Keywords:

Two-photon absorption

Organic dyads

H-bonding effect

Proton transfer

Excited state

ABSTRACT

New near-infrared two-photon absorption π -extended benzotriazole–coumarin dyads as target molecules were synthesized. The corresponding coumarin derivatives and esterified dyads were also prepared as the references. The experimental evidence of internal proton transfer in the excited state of the benzotriazole-based chromophores under one and near-infrared two-photon irradiation are firstly presented in this Letter.

© 2014 Elsevier Ltd. All rights reserved.

There is a long-staying scientific controversy on internal proton transfer in the excited state for *o*-hydroxy-phenyl-benzotriazole family, which contains typical intramolecular proton transfer groups. Unlike *o*-hydroxy-phenyl-benzothiazole and *o*-hydroxy-phenyl-benzoxazole,^{1,2} excited state intramolecular proton transfer (ESIPT) of *o*-hydroxy-phenyl-benzotriazole family is lack of the substantial experimental evidence. Due to more electron-deficiency in the heterocyclic ring of *o*-hydroxy-phenyl-benzotriazole comparing with *o*-hydroxy-phenyl-benzothiazole and *o*-hydroxy-phenyl-benzoxazole, the occurrence of internal proton transfer in the excited state of *o*-hydroxy-phenyl-benzotriazole family decreases.

So far, there have been different opinions on the occurrence of internal proton transfer in the excited state for this family.^{3–5} For instance, it was reported that intramolecular electron transfer led to the deactivation of the excited state for *o*-aryl-benzotriazoles,³ while internal proton transfer was regarded as the main decay pathway in the excited singlet state for 2-(2'-hydroxy-phenyl)-benzotriazole.^{4,5}

Two-photon absorption (TPA) chromophores opened a door for the application of near-IR laser,^{6–8} which demonstrated various superior physical advantages such as low energy, deep penetration, and negligible damage to normal biological tissues. A few 2-(2'-hydroxyphenyl)-benzoxazole-based dyes with TPA cross sections

were reported to exhibit ESIPT under near-IR laser excitation.⁹ Unfortunately, no characteristic proton transfer emission band was detected under near-IR laser irradiation to these benzoxazole-based dyes. To the best of our knowledge, there is no report on ESIPT of *o*-hydroxy-phenyl-benzotriazole-based organic chromophores under one-photon and near-IR laser irradiation.

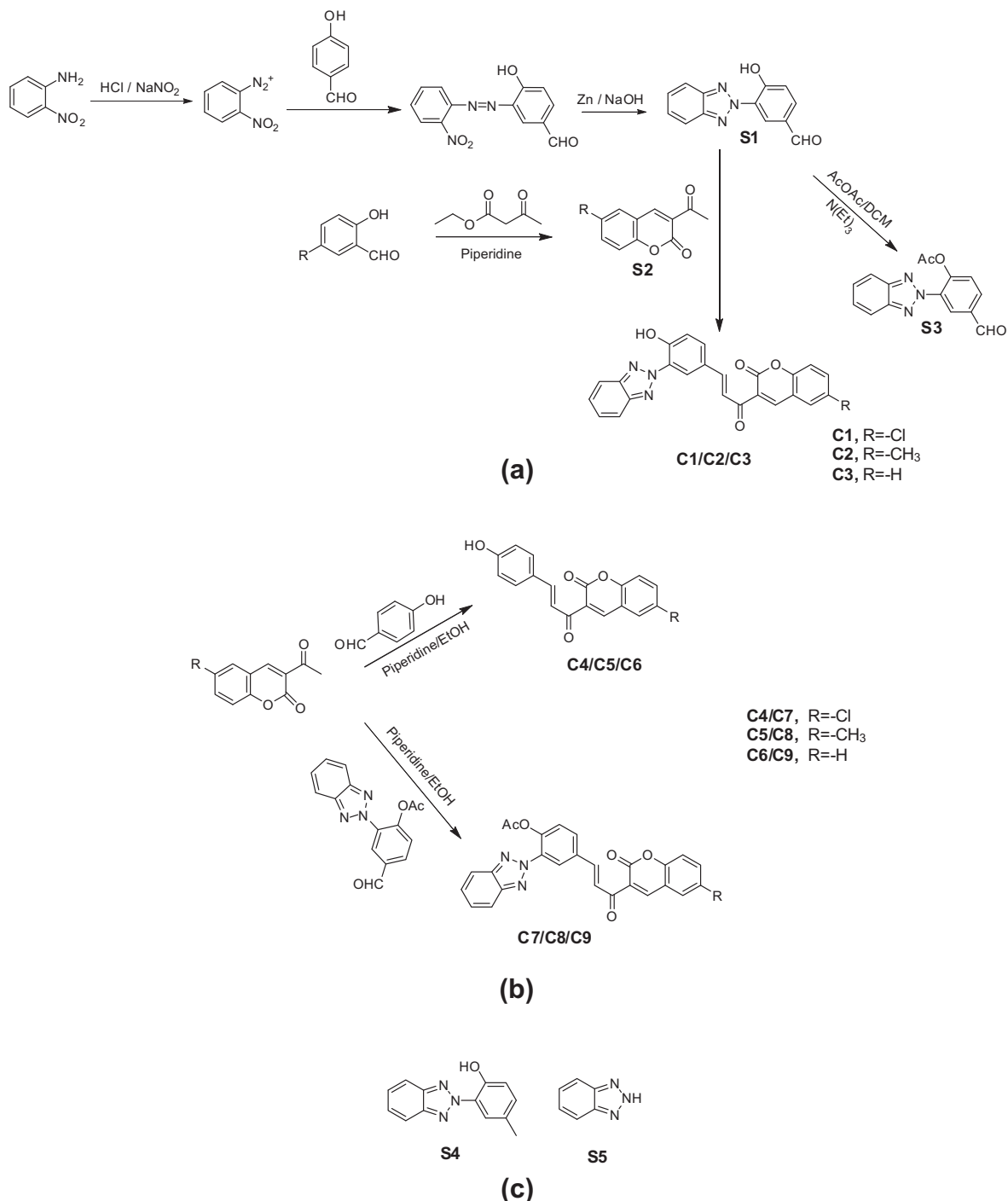
Extended organic chromophores with ESIPT possess more application potentials.^{10,11} In particular, π -extended organic chromophores with ESIPT can be utilized as TPA dyes by near-IR femtosecond laser. Several groups developed enlarged organic molecules containing proton transfer segments through the chemical covalent bond.^{12–14} However, the insertion of π -conjugation units was reported to inhibit intramolecular proton transfer in the excited state for an organic chromophore.¹² Therefore, the development of new π -extended *o*-hydroxy-phenyl-benzotriazole-based organic chromophores with internal proton transfer in the excited state is still a great challenge.

In this Letter, coumarin is used as the π -unit to construct new benzotriazole–coumarin dyads, where the electron-accepting α,β -unsaturated carbonyl group acts as the π -linker to increase the activity of the phenolic hydroxy group. Herein, we describe our studies on the internal proton transfer of 2-(2'-hydroxy-phenyl)-benzotriazole–coumarin dyads in the excited state under both one-photon and near-IR two-photon irradiation, respectively.

Several target benzotriazole–coumarin dyads (**C1–C3**) were designed and synthesized as shown in **Scheme 1**. The corresponding coumarins (**C4–C6**) and *O*-acetyl dyads (**C7–C9**) were also prepared

* Corresponding authors. Tel./fax: +86 23 65102531.

E-mail addresses: zpluo@126.com (Z. Luo), hongruli1972@gmail.com (H. Li), fanggao1971@gmail.com (F. Gao).



Scheme 1. Chemical structures of the molecules studied in this work.

for reference. The detailed procedures for the target and reference molecules are described in [Supplementary material](#).

As shown in ¹H NMR (Fig. 1), the chemical shift of OH in **C1** moves to downfield comparing with those of **C4** and phenol in D⁶-DMSO (**C1**, 11.23 ppm, **C4**, 10.20 ppm, phenol, 9.35 ppm). It is also noticed that ¹H NMR chemical shift of OH in the equal molar mixture of **C4**/1,2,3-benzotriazole (**S5**) is almost the same as that of **C4** (Fig. S1, [Supplementary material](#)). In addition, ¹H NMR chemical shift of OH in the equal molar mixture of **C7**/phenol is almost the same as that of phenol (Fig. S1).

Compounds **C2** and **C3** exhibit similar ¹H NMR nature as **C1**. ¹H NMR chemical shift of OH in **C2** or **C3** situates at downfield comparing with those of **C5** or **C6** in D⁶-DMSO. ¹H NMR chemical shift of OH in the equal molar mixture of **C5**/1,2,3-benzotriazole or **C6**/1,2,3-benzotriazole is almost identical to that of **C5** or **C6**, respectively. Furthermore, ¹H NMR chemical shift of OH in the equal molar mixture of **C8**/phenol or **C9**/phenol is similar to that of phenol, respectively.

The above results also show that there is no strong interaction between OH and C=N groups in the ground state as they are contained in different molecules respectively. The fact that ¹H

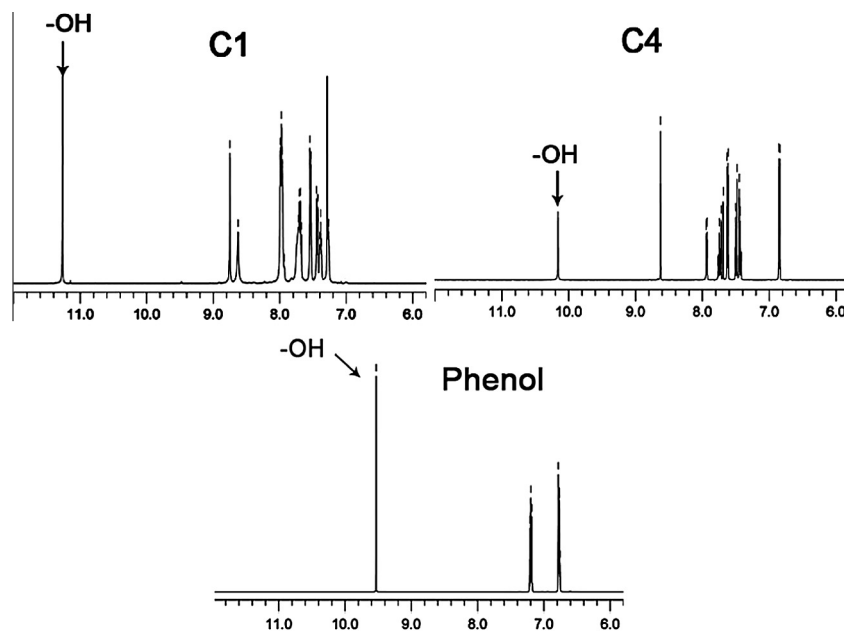


Figure 1. ^1H NMR spectra of **C1**, **C4**, and phenol.

NMR chemical shifts of OH in target molecules **C1–C3** appeared at lower magnetic field suggests that there is an intramolecular H-bonding effect between the OH and the C=N group in the ground states of **C1–C3** respectively.¹⁵

Comparing with the target molecules, ^1H NMR chemical shift of OH in 4-methyl-2-(2*H*-benzotriazol-2-yl)-phenol (**S4**) is located at the upfield (Fig. S1). This reflects the electron-withdrawing effect of the α,β -unsaturated carbonyl group on internal H-bonding role in the ground state.

By comparison of the ^1H NMR of **C1**, **C2**, and **C3**, the chemical shift of OH in **C1** moves to lower magnetic field (**C1**, 11.23 ppm, **C2**, 11.19 ppm, and **C3**, 11.15 ppm), indicating that there is stronger internal H-bonding effect in the ground state of **C1**.

The ultraviolet/visible absorption spectra of the target and reference molecules were determined in various solvents. Typical absorption spectra of **C1**, **C4**, and **C7** in benzene and DMF are shown in Figure 2a and b, respectively. Because 1,2,3-benzotriazole shows quite weak optical density, coumarin moiety makes a major contribution to the absorption of the entire chromophore molecule. As a result, the maximal molar extinction coefficients and the absorption maxima of **C1** and **C4** are quite close (such as in benzene, **C1**, λ_{max} , 361 nm, ϵ_{max} , $0.208 \text{ cm}^{-1} \text{ mol}^{-1} \text{ L}$, **C4**, λ_{max} , 355 nm, ϵ_{max} , $0.242 \text{ cm}^{-1} \text{ mol}^{-1} \text{ L}$, Table 1).

C1, **C4**, and **C7** only exhibit the absorption in the range of 250–450 nm in benzene (Fig. 2a). While in DMF, in addition to the absorption in the above range, **C1** shows one more new absorption band in the range of 450–700 nm (Fig. 2b). Similar absorption phenomenon is also observed in DMSO. As contrast, the reference molecules such as **C4** and **C7** only show the absorption in the range of 250–420 nm in various solvents. The further study shows that the equal molar mixture of **C4**/1,2,3-benzotriazole and **C7**/phenol do not display the absorption in the range of 450–700 nm in DMF and DMSO, respectively, (Fig. S2, Supplementary materials).

The results suggest that the new absorption band is not originated by intermolecular interaction. The absorption of **C1** in 450–700 nm in DMSO and DMF is assigned to internal molecular H-bonding effect.³ It is considered that the great polarity of DMSO and DMF is beneficial for the enhancement of the activity of the hydroxy group,¹⁶ so intramolecular hydrogen bonding strength of **C1** between the hydroxy group and imino group increases, while leading to the formation of the absorption band in 450–700 nm.

Therefore, it is noticed that the absorption band of **C1** in the range of 450–700 nm gradually decreases when lower polar solvents such as CH_2Cl_2 is added into DMF or DMSO solution (Fig. S3, Supplementary materials).

The study shows that the absorption of **C1** in the range of 450–700 nm decreases in triethylamine (TEA) comparing with that

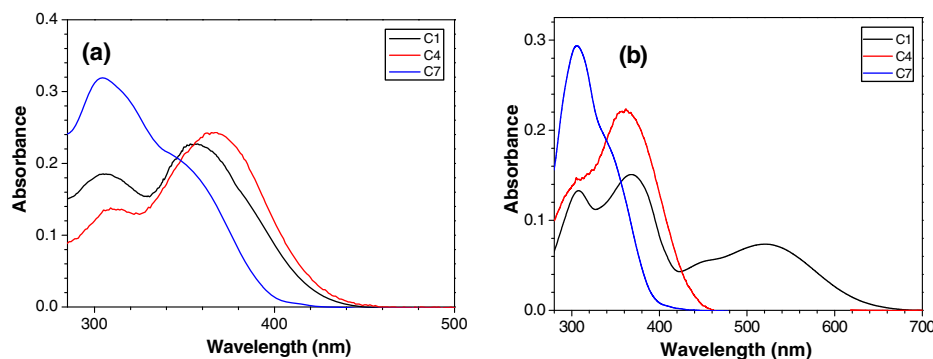


Figure 2. UV/visible absorption spectra (a) and (b) of **C1**, **C4**, and **C7** in benzene and DMF, respectively, the concentration is 10^{-5} mol/L for the absorption spectra.

Table 1

The spectral parameters of **C1**, **C4**, and **C7** in various solvents, $\lambda_{a,max}$: the absorption maximum (nm), $\lambda_{f,max}$: the emission maximum (nm), ϵ_{max} , the maximal molar extinction coefficient ($\text{cm}^{-1} \text{mol}^{-1} \text{L}$), Φ , the fluorescence quantum yield

Solvents	C1				C4				C7			
	$\lambda_{a,max}$ (nm)	$\lambda_{f,max}$ (nm)	Φ	$\epsilon_{max} (\times 10^{-5})$	$\lambda_{a,max}$ (nm)	$\lambda_{f,max}$ (nm)	Φ	$\epsilon_{max} (\times 10^{-5})$	$\lambda_{a,max}$ (nm)	$\lambda_{f,max}$ (nm)	Φ	$\epsilon_{max} (\times 10^{-5})$
Benzene	361	431	0.081	0.208	360	431	0.016	0.242	365	439	0.060	0.268
THF	359	431	0.080	0.276	360	438	0.025	0.256	373	434	0.070	0.289
EtOAc	351	433	0.105	0.291	351	403	0.121	0.107	368	429	0.151	0.293
CH_2Cl_2	354	444	0.093	0.265	355	434	0.015	0.275	360	432	0.115	0.285
Acetone	333	450	0.080	0.175	336	435	0.013	0.168	363	433	0.104	0.099
CH_3CN	344	448	0.077	0.320	350	436	0.011	0.324	354	437	0.054	0.270
DMSO	381	425	0.010	0.245	382	433	0.006	0.237	340	434	0.091	0.298
DMF	373	419	0.013	0.148	383	430	0.007	0.221	359	413	0.093	0.195
Methanol	307	432	0.007	0.152	353	435	0.009	0.197	377	435	0.013	0.325

in DMSO or DMF (Fig. S4, Supplementary materials). As a matter of fact, that absorption decreases as well when aqueous potassium carbonate solution is added (Fig. S5, Supplementary materials). This could be the result of partial neutralization of the hydroxy group by TEA or potassium carbonate, and intramolecular hydrogen bonding effect in **C1** decreases. It is further observed that the diminished absorption in 450–700 nm is recovered as the further addition of aqueous HCl solution.

Compounds **C2** and **C3** show the similar absorption spectral properties as **C1**. In lower polar solvents comparing with DMSO and DMF, **C2**, and **C3** only display the absorption below 450 nm. In contrast, **C2** and **C3** exhibit one more new absorption band above 450 nm in DMSO and DMF, respectively.

The further investigation also shows that the absorption band of **C1** in 450–700 nm decreases in methanol (Fig. S6, Supplementary materials), and it nearly disappears for **C2** and **C3**. The results show that intermolecular H-bonding effect between the methanol molecules and the solute molecules inhibit internal H-bonding effect in these target chromophores. The results also indicate that **C1** displays stronger internal H-bonding effect than **C2** and **C3**.

Normally, internal H-bonding effect in the ground state of an organic molecule is considered as the prerequisite to undergo intramolecular proton transfer in the excited state. Hence, the presence of internal H-bonding effect in the target molecules **C1–C3** means that intramolecular proton transfer in the excited state can occur. The fluorescence spectra of the molecules were measured in various solvents to get the experimental evidences of internal proton transfer in the excited singlet state.

Typical linear fluorescence emission spectra of **C1**, **C4**, and **C7** in benzene and DMF are shown in Figure 3. In benzene, **C1**, **C4**, and **C7** show single emission band in 380–600 nm, and the maximal emission wavelengths are close (Table 1, **C1**, 361 nm, **C4**, 360 nm, and **C7**, 365 nm). In DMF, **C4** and **C7** still show single emission band in 380–600 nm. In contrast, **C1** exhibits dual emission bands in 380–700 nm in DMF.

In DMF, the maximal emission wavelength of the first emission band of **C1** is close to those of **C4** and **C7** (ca. 430 nm). The maximal wavelength of the second emission band of **C1** is much red-shifted (100 nm, in DMF), and the second emission band possesses large Stokes shift (140 nm, in DMF). Similar experimental phenomena are also observed in DMSO. In lower polar solvents such as benzene and CH_2Cl_2 comparing with DMSO and DMF, **C1** shows only single emission band in 380–600 nm. However, **C4** and **C7** exhibit the similar single emission band in 380–600 nm in various solvents.

The equal molar mixtures of **C4/S5** and **C7/phenol** also show the single emission band in 380–600 nm as **C4** and **C7** in various solvents (Fig. S7, Supplementary materials). This shows the second emission band of **C1** in DMF is not yielded by intermolecular interaction. It is found that the new emission band in 480–700 nm of **C1** gradually decreases as lower polar solvents such as CH_2Cl_2 is added to DMSO or DMF (Fig. S8, Supplementary materials). In TEA, the second emission band in 480–700 nm greatly decreases (Fig. S9, Supplementary materials). It is further observed that the second emission band in 480–700 nm in DMF and DMSO solution also decreases as aqueous potassium carbonate solution is added (Fig. S10, Supplementary materials). On the other hand, the reduced second emission band by base is recovered as aqueous HCl solution is added.

Compounds **C4** and **C7** also exhibit normal Stokes shift in various solvents as shown in Table 1 (such as 70 nm in benzene). The first emission band of **C1** in DMSO and DMF exhibits a similar Stokes shift (44 nm in DMF and 46 nm in DMSO). The results suggest that the first emission band of **C1** in DMSO and DMF is from the normal enol^{*} to enol decay, which is almost effectively the same as $S_0 \rightarrow S_1$ normal absorption spectral feature.¹⁷ However, the second emission band possessing larger Stokes shift (such as 140 nm in DMF) is ascribed to internal proton transfer in the excited state (keto^{*} to keto decay, Scheme 2).¹⁸ It is considered that ESIPT means the occurrence of real chemical reaction, and thus polar organic solvents such as DMSO and DMF

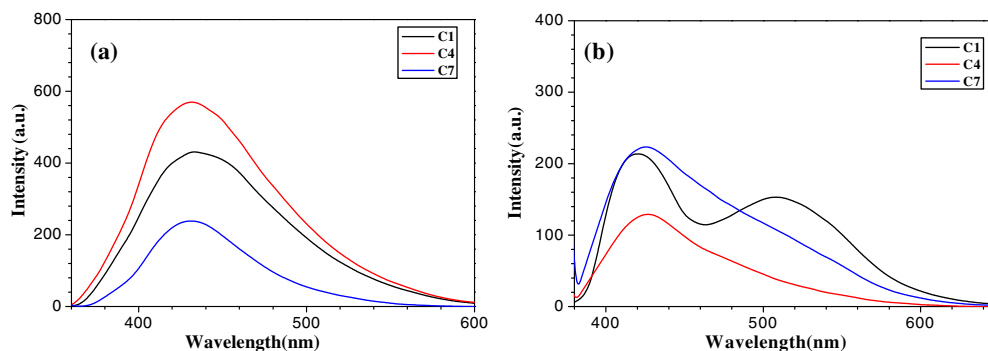
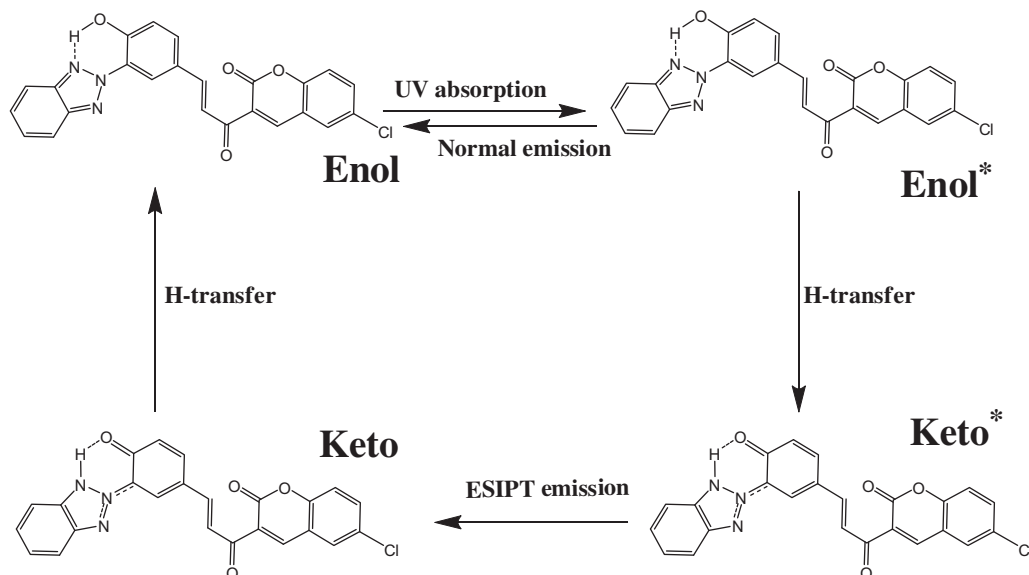


Figure 3. Emission spectra (a) and (b) of **C1**, **C4**, and **C7** in benzene and DMF, respectively, the concentration is $5 \times 10^{-6} \text{ mol/L}$ for the emission spectra, excitation at 350 nm.



are favorable for the realization of such process.¹⁹ However, the hydroxy group in **C1** can be neutralized by TEA or potassium carbonate. Thus, internal proton transfer in the excited state of **C1** is inhibited by TEA or potassium carbonate, and the second emission band in 480–700 nm decreases.

Compounds **C2** and **C3** show the similar linear emission spectral properties as **C1**. It suggests that the target dyads **C1–C3** can undergo intramolecular proton transfer in DMSO and DMF in the excited state. The further determination shows that the second emission band of the target dyads **C1–C3** in 480–700 nm decreases in methanol (Fig. S11, Supplementary materials). The results suggest that intermolecular H-bonding effect between the solvents and the solute inhibits intramolecular proton transfer in the excited state of these target molecules.¹⁷

It is observed that I_{E^*}/I_{N^*} ratio (the ratio of the maximal internal proton transfer emission intensity to the maximal normal emission intensity) of **C1** in DMF is higher than in DMSO (DMF, 0.820, DMSO, 0.381). **C2** and **C3** exhibit the same phenomena as well. This can be ascribed to the high polarity in DMF, which favors internal proton transfer in the excited state of benzotriazole-coumarin dyads.

It is also noticed that I_{E^*}/I_{N^*} ratio of **C1** is greater than those of **C2** and **C3** in DMSO or DMF respectively (such as in DMF, **C1**, 0.820, **C2**, 0.470, and **C3**, 0.684), which can be ascribed to more intensive

H-bonding effect due to electron-withdrawing effect of the chlorine group in the coumarin ring of **C1**.

The target dyads **C1–C3** exhibit TPA upconverted fluorescence emission under near-IR femtosecond laser excitation. Typical TPA fluorescence emission spectra of **C1**, **C4**, and **C7** in benzene and DMF under 730 nm laser are shown in Figure 4. It is surprising that **C1** shows dual TPA emission bands in the range of 400–700 nm in both benzene and DMF solvents, which is different from the linear emission nature. However, **C4** and **C7** still display single emission band in the range of 400–600 nm under near-IR laser irradiation. Further study shows that the mixture of **C4**/1,2,3-benzotriazole or **C7**/phenol exhibits the same TPA emission spectra as **C4** or **C7**, respectively, (Fig. S12, Supplementary materials). In other solvents, **C1** exhibits dual emission bands 400–700 nm as excited by 730 nm femtosecond laser as well. **C4** and **C7** show single emission band from 400 to 600 nm in various solvents.

The maximum emission wavelength of the first TPA emission band of **C1** is close to those of **C4** and **C7** (ca. 450 nm) in various solvents. The maximal wavelength of the second emission band of **C1** under near-IR laser irradiation is similar to that of one-photon excitation (ca. 540 nm). The second TPA emission band of **C1** from 500 to 700 nm decreases in TEA. The addition of aqueous potassium carbonate into DMSO or DMF solution also causes the diminishment of the second TPA emission band, which is recovered

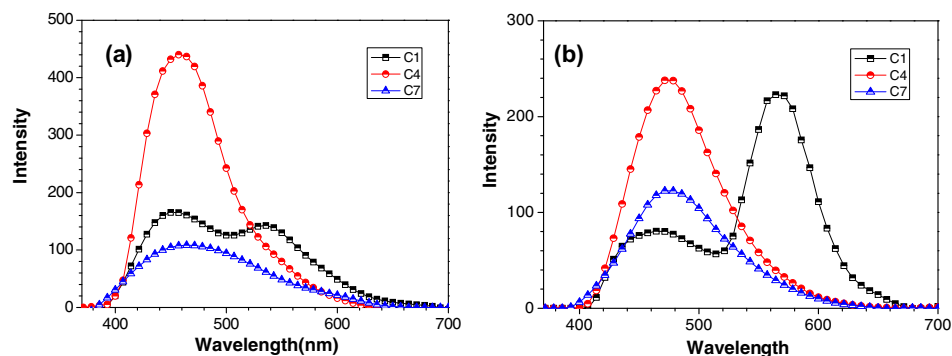


Figure 4. TPA fluorescence emission spectra (a) and (b) of the partners **C1**, **C4**, and **C7** in benzene and DMF respectively under 730 nm femtosecond laser irradiation, the concentration is 5×10^{-4} mol/L.

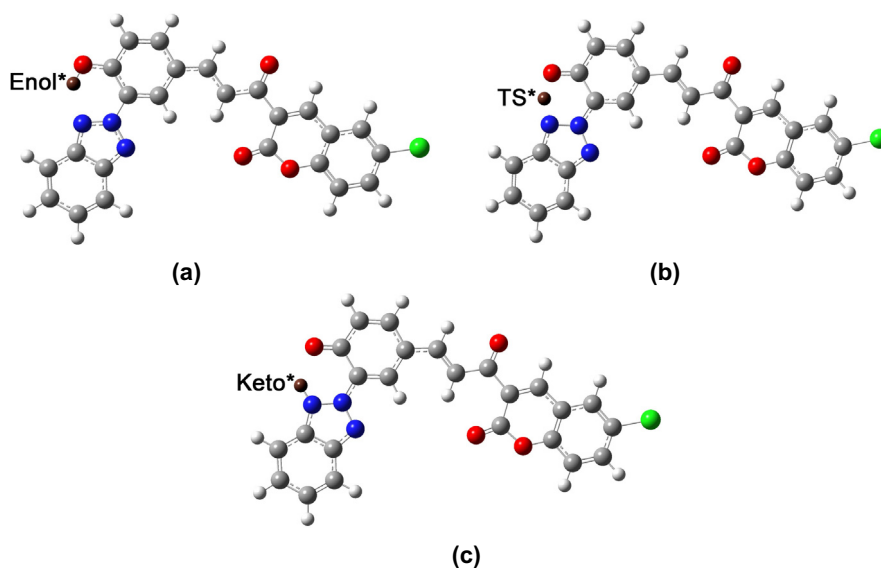


Figure 5. Optimized geometries of enol (a), TS (b), and keto (c) forms of **C1** by Gaussian 09 program package.

as aqueous HCl solution is further titrated (Fig. S13, Supplementary materials).

The results suggest that the first emission band of **C1** is TPA normal decay process, and the second emission band is TPA ESIPT process. The same phenomena are also shown by **C2** and **C3**. The results suggest that **C1**, **C2** and **C3** are able to undergo ESIPT under femtosecond near-IR laser irradiation, while **C4–C9** can not show these properties.

It is interesting that I_{E^*}/I_{N^*} ratio in TPA emission spectra of **C1** is much higher than that in one-photon emission in DMSO and DMF (such as in DMF, for **C1**, 2.92, **C2**, 1.91, and **C3**, 2.42). Even in methanol, **C1** exhibits competitive ESIPT emission excited by 730 nm femtosecond laser as well (I_{E^*}/I_{N^*} , 1.18 in methanol, Fig. S14 Supplementary materials). This shows that ESIPT emission becomes the primary deactivation route of the excited states of **C1** under near-IR femtosecond laser excitation.¹⁷ Compounds **C2** and **C3** show similar experimental phenomena under near-IR laser irradiation.

It is accepted that intramolecular phototautomerization process between enol and keto tautomers in the excited state of an organic molecule may be finished in femtosecond time scale,²⁰ which matches well with near-IR femtosecond pulsed laser. Hence, ESIPT becomes predominant pathway to deactivate the excited states of **C1** during femtosecond near-IR induced two-photon process.

It is further noticed that benzotriazoles derivatives **S1** and **S4** do not emit TPA fluorescence emission under near-IR femtosecond laser irradiation. This shows that **S1** and **S4** possess small TPA ability, and coumarin part makes a major contribution to TPA of the target dyads.

The transition state (TS) from enol to keto in the excited state of the target molecules is further revealed by molecular geometry optimization. The representative optimized geometries of enol, TS, and keto forms of **C1** in the excited state are shown in Figure 5, which clearly suggests the **C1** undergoes active hydrogen atom transfer process from enol to keto in the excited state.

To be summarized, this Letter firstly reports some new benzotriazole–coumarin dyads. It is demonstrated that internal H-bonding effect is presented in these new π -extended benzotriazole–coumarin dyads on the basis of the analysis of ¹H NMR spectra and the UV/visible absorption spectra. Intramolecular proton transfer in the excited state of π -extended *o*-hydroxy-phenyl-benzotriazole–coumarin dyads is firstly revealed by well-separated

dual emission spectra under one-photon and near-infrared two-photon irradiation. Furthermore, ESIPT becomes predominant decay pathway in the excited states of the target dyads as irradiated by near-IR femtosecond laser. The results presented in the work would be much beneficial for the development and application of new near-infrared two-photon benzotriazole-based organic chromophores with ESIPT.

Acknowledgements

This work was financially supported by CSTC2012jjB50007 and CSTC2010BB0216. H. Li is grateful to the Postdoctoral Science Foundation of China for their encouraging supporting (Grants 22012T50762 & 2011M501388). L.Y. also thanks Graduate Student Innovation Foundation of Chongqing University (CDJX11131146). We greatly appreciate Key Laboratory of Photochemical Conversion and Optoelectronic Materials, CAS for the help in the laser detection.

Supplementary data

Supplementary data (the synthesis of the molecules, NMR spectra as well as optical spectra) associated with this article can be found, in the online version, at <http://dx.doi.org/10.1016/j.tetlet.2014.11.074>.

References and notes

- Itoh, M.; Fujiwara, Y. *J. Am. Chem. Soc.* **1985**, *107*, 1561.
- Liu, Z.; Zhang, C.; Li, Y.; Wu, Z.; Qian, F.; Yang, X.; Guo, Z. *Org. Lett.* **2009**, *11*, 795.
- Maliakal, A.; Lem, G.; Turro, N.; Ravichandran, R.; Suhadolnik, J.; DeBellis, A.; Wood, M.; Lau, J. *J. Phys. Chem. A* **2002**, *106*, 7680.
- Waiblinger, F.; Keck, J.; Stein, M.; Fluegge, A.; Kramer, H.; Leppard, D. *J. Phys. Chem. A* **2000**, *104*, 1100.
- Keck, J.; Kramer, H. E. A.; Port, H.; Hirsch, T.; Fischer, P.; Rytz, G. *J. Phys. Chem.* **1996**, *100*, 14468.
- Mongin, O.; Brunel, J.; Porrès, L.; Blanchard-Desce, M. *Tetrahedron Lett.* **2003**, *44*, 2813.
- Belfield, K. D.; Hagan, D. J.; Van Stryland, E. W.; Schafer, K. J.; Negres, R. A. *Org. Lett.* **1999**, *1*, 1575.
- Kim, S.; Ohulchanskyy, T. Y.; Pudavar, H. E.; Pandey, R. K.; Prasad, P. N. *J. Am. Chem. Soc.* **2007**, *129*, 2669.
- Tian, Y.-Q.; Chen, C.-Y.; Yang, C.-C.; Young, A.-C.; Jang, S.-H.; Chen, W.-C.; Jen, A. K.-Y. *Chem. Mater.* **2008**, *20*, 1977.
- Wu, Y.-K.; Peng, X.-J.; Fan, J.-L.; Gao, S.; Tian, M.-Z.; Zhao, J.-Z.; Sun, S.-G. *J. Org. Chem.* **2007**, *72*, 62.

11. Tang, K.; Chang, M.; Lin, T.; Pan, H.; Fang, T.; Chen, K.; Hung, W.; Hsu, Y.; Chou, P. *J. Am. Chem. Soc.* **2011**, *133*, 17738.
12. Zhao, J.; Ji, S.; Chen, Y.; Guo, H.; Yang, P. *Phys. Chem. Chem. Phys.* **2011**, *14*, 8803.
13. Chu, Q.; Medvetz, D. A.; Pang, Y. *Chem. Mater.* **2007**, *19*, 6421.
14. Lin, C.; Chen, C.; Chuang, M.; Chen, Y.; Chou, P. *J. Phys. Chem. A* **2010**, *114*, 10412.
15. Gilli, P.; Bertolasi, V.; Ferretti, V.; Gilli, G. *J. Am. Chem. Soc.* **2000**, *122*, 10405.
16. Nazie, H.; Yildiz, M.; Yilmaz, H.; Tahir, M.; Ulku, D. *J. Mol. Struct.* **2000**, *524*, 241.
17. Gao, F.; Wang, X.; Li, H.; Ye, X. *Tetrahedron* **2013**, *69*, 5355.
18. Lim, S. J.; Seo, J. G.; Park, S. Y. *J. Am. Chem. Soc.* **2006**, *128*, 14542.
19. Nazir, H.; Yildiz, M.; Yilmaz, H.; Tahir, M.; Padalkar, V.; Tathe, A.; Gupta, V.; Patil, V.; Phatangare, K.; Sekar, N. *J. Fluoresc.* **2012**, *22*, 311.
20. Hsieh, C.; Cheng, Y.; Hsu, C.; Chen, K.; Chou, P. *J. Phys. Chem. A* **2008**, *11*, 8323.